2013

Combining High Speed Imaging And Acoustic Emission Analysis For Crack Growth In Thick Samples

Jr. Michael Gillespie
North Carolina Agricultural and Technical State University

Combining High Speed Imaging and Acoustic Emission Analysis for Crack Growth in Thick Samples

Michael E. Gillespie Jr.

North Carolina A&T State University

A thesis submitted to the graduate faculty

in partial fulfillment of the requirements for the degree of

MASTER OF SCIENCE

Department: Mechanical Engineering

Major: Mechanical Engineering

Major Professor: Dr. Mannur Sundaresan

Greensboro, North Carolina

2013

The Graduate School
North Carolina Agricultural and Technical State University
This is to certify that the Master's Thesis of

Michael E. Gillespie Jr.

has met the thesis requirements of
North Carolina Agricultural and Technical State University

Greensboro, North Carolina
2013

Approved by:

Dr. Mannur Sundaresan
Major Professor

Dr. Albert Esterline
Committee Member

Dr. Trisha Sain
Committee Member

Dr. Samuel Ofori
Department Chair

Dr. Sanjiv Sarin
Dean, The Graduate School

Biographical Sketch

Michael E. Gillespie Jr. was born to Mr. Michael Gillespie Sr. and Mrs. Millicent Roseboro on November 9th, 1987 in Statesville, North Carolina. He has two sisters, Sierra and Yana, and one brother, Ekiah. Michael is engaged to be married next year to Nacole Lilly

He received his Bachelor of Science degree in Engineering Mathematics from Saint Augustine's College in Raleigh, North Carolina. He is now a candidate for the Master of Science degree in Mechanical Engineering from North Carolina Agricultural and Technical State University

Dedication

I dedicate this work to memory of my grandmother, Katheryn McClelland. I thank you for always believing in me no matter what. I love you, may you watch over me while you rest in peace.

Acknowledgements

I would like to thank Dr. Mannur Sundaresan for giving me the opportunity to continue and pursue a higher education here at North Carolina A&T State University. Thank you for being a leader and knowledge over the course of my education. I would also like to thank Dr. Jim Blackshire, SOCHE, and the entire materials branch of WPAFB for their assistance, resources, and dedication to helping me fulfill my goal of attaining a master's degree. Last but not least I would like to acknowledge and give thanks to my colleagues and lab members for their assistance over the years.

Table of Contents

List of Figures

List of Tables

Abstract

Over 80% of components in a system that undergo fatigue cycling fail due to cracking. Acoustic emission (AE) has become a major resource in non-destructive testing (NDT) for the detection, location, and quantification of cracking events. Normally, AE an event is referred to as crack growth, fretting, or friction. As an AE signal progress through material, the waveform converts into several modes; additionally, attenuation and dispersion may also change the waveform. Furthermore, the noise may intrude into the signal in such a way that by time the signal from the source arrives at the sensor the waveform becomes very complex. Due to the complexity of the signal, the source of the acoustic emission event is very difficult to determine.

In the following research, the aim is to develop relationships between signal content and high-speed digital imaging to assist in determining key components of the AE source. Thick aluminum bar samples are experimentally subject to cyclic loading utilizing three point bending setup to observe the crack growth. The crack growth thus generated is monitored simultaneously with the help of a high-speed camera system to record the expansion of the crack tip, and by piezoelectric (PZT) sensors bonded over the specimen surface to collect the AE signals. Analysis is provided to differentiate between the AE signals occurring due to crack growth and fretting occurring during the closing of the crack. Furthermore, a 3D model was studied to differentiate between surface and interior crack growth signals. The fracture results show clear indication of the interior crack growth propagating at a different rate to the crack growth along the free surface of the specimen. This phenomenon is attributed to the plane stress and plane strain conditions in the specimen. This important result comes from the video recordings showing the future of the crack path as it propagates over the surface.

CHAPTER 1

Introduction

1.1 Non-Destructive Evaluation

Structures or the components of a system that undergo stress are subjected to some type of deformation at some point within its service life. The deformation could be minor, they could be major, but it is up to scientist and engineers to find an analysis to detect such an event. NDE is the study of evaluating a system or the components of a system for discontinuities or differences in material characteristics without disabling the usage of that system or the components of the system. Non-destructive testing (NDT), a term closely related to NDE, has emerge over destructive testing due to destructive testing methods destroy the sample which could limit the amount of samples that can be tested and could become very costly. Destructive tests are often used to determine the physical properties of materials such as ductility, yield strength, ultimate tensile strength, fracture toughness and fatigue strength. The NDT method focuses more on the material properties and characteristics that will affect the serviceability of the component or system. The different NDT methods include ultrasonic, radiographic, thermographic, electromagnetic, optic, and visualization. The NDT technique that will be discussed in this research is under the method of ultrasonic, acoustic emission (AE).

1.2 Structural Health Monitoring

Emerging from NDE, structural health monitoring (SHM) has become a vital necessity in monitoring the safety and serviceability of critical structures throughout the world. While NDE detects defects after the fact, SHM systems use sensor technology to record real time information to relay information about the structure. The importance and main objective for this type of system is to provide information about the initiation of damage or deformation in the system.

Scientist and engineers have been focusing on this area or research to improve the life of structures, decrease cost of replacing or servicing components of structures, and for the greatest reason, saving the lives of the people. SHM can be broken down into 3 elite categories;

1. Detection- Notification that there exist damage in the system
2. Location- Determining the location of the damage
3. Quantification- Classifying the severity of this damage

An abundance of research, principles, and techniques have been published and accepted in the first two categories, therefore, majority of those working in the SHM field are concentrated on excelling in quantification. Once the damage is detected and located, can we use the information detained to tell us the physical characteristics and/or the life expectancy of the system? This research will use the passive monitoring method of acoustic emission to assist in quantifying crack growth events in thick aluminum bar samples.

1.3 Acoustic Emission

AE has been around for centuries and a lot of research has been published to understand and define this technique. AE is defined as propagation of elastic waves caused by a rapid release of energy resulting from small displacement caused by an external force. The release of stress waves can be generated from various types of sources such as:

a. Twinning

b. Grain boundary sliding and rotation

c. Slip band formation

d. Dislocation unpinning and motion

e. Plastic deformation at a stress concentration

f. Void initiation and growth

g. Crack initiation and propagation

h. Fretting or friction

When an AE event (the release of stress waves) occurs, energy is radiated in all direction, propagating with a curvature wave front. Therefore, the further the detection is away from the source, the less the energy will be in the signal detected. The signal is detected by a sensor bonded or mounted to the surface of the material, which is amplified by an amplifier to be recorded by the data acquisition system. This process is shown figure below.

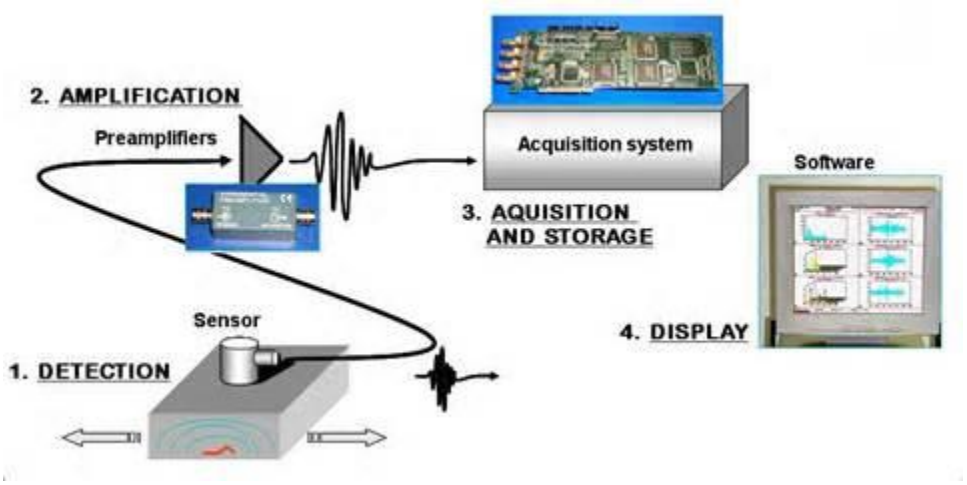

Figure 1. The AE process

The highest area of interest in AE monitoring is interpreting the detected complex signal waveforms in a way to extract helpful information that will quantify the event. Its priority for NDE to develop an integrated and robust structural health monitoring (SHM) system that will improve public safety by monitoring the safety of systems by alerting minor and major damages and improving the cost of maintenance of large structures or systems. NDT, structural health monitoring, and AE all come down to one final goal and that is quantification. Being able to quantify the event, determine the size, length, debt, condition, and its overall effect on the system is where the bulk of research is now allocated for AE. Over the last 2 decades, the analysis of AE

has been developed and used for various applications: including analyzing the damages in fiber and textile composites (Ares J. Rosakis, 1999), pressure vessel testing (Palmer, 1973), crack detection in welding (Karlsson, 2010), monitoring erosion-corrosion (Mohamed SHEHADEH [1], 2012), and structural health monitoring for aircraft material (Pullin et al., 2010). AE technology is a great asset for SHM but it is restricted by the lack of predictive modeling capability and quantitative source characteristic information.

1.4 Background

There are numerous factors that may affect AE signals as they propagate through the material or the structure. As stated previously, there are also numerous sources of acoustic emission. There are defined parameters that can be analyzed from AE signals but as of today, there are not many theories that separate the different types of AE signals from different sources. For example, when applying AE to three point bend test, within 100 cycles there may be 1000 signals detected and recorded. The sources of these signals could originate from friction between the bend bars and the specimen (friction), crack growth, electrical noise, or from fretting shown in the figure below.

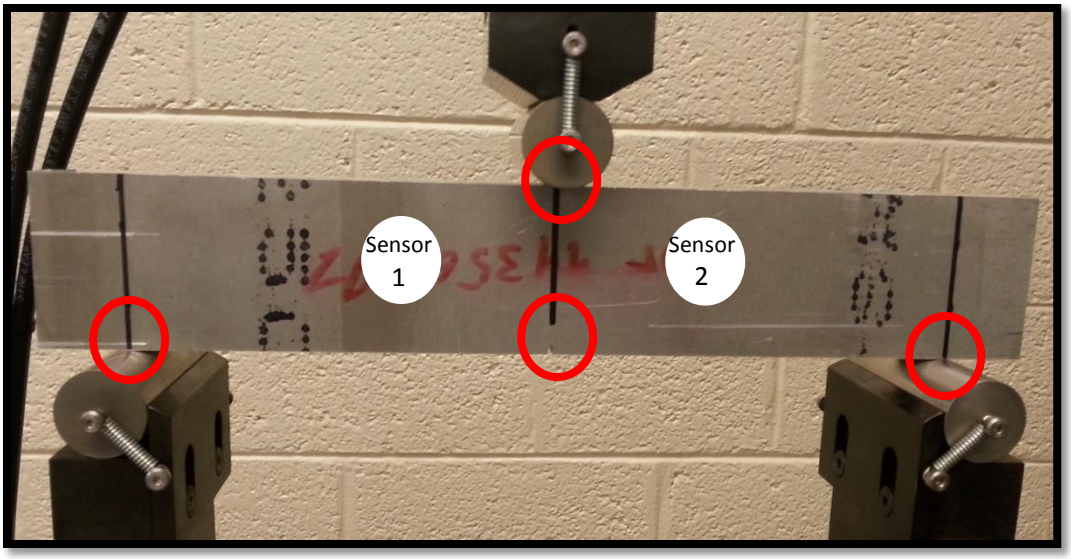

Figure 2. Areas where AE events may occur

In dealing with the crack growths alone, AE signal events could come from the interior of the material or from the surface of the material. This lack of knowledge has sufficiently crutched the advancement of AE technology. If certain characteristics from the signal could be directly correlated to the known source of acoustic emission then it would enable engineers to better quantify the AE event. At an even higher advantage, if the damage that is occurring could be physically seen while it is occurring, other parameters could assist into analyzing the signal such as velocity. It all comes down to what is the AE source? Can we determine what the AE source signal looks like before it is altered by noise or material properties? This research aims to assist in correlating AE signals with the known AE source with the use of high-speed imaging, AE signal analysis, and finite element modeling.

1.5 Objectives

The general objective of this research is to identify key parameters for better quantification of AE signals. The specific objectives include;

- **Capturing surface crack growth using a high-speed camera**

Capturing a crack growth on video along the surface of the bar sample will assist with two things; indicate visual crack growth phenomena and determine the crack growth velocity.

- **Correlate AE signals with video**

Crack growth velocity and the crack growth length may change key parameters within the AE to indicate defined characteristics of the source

- **Use PZ FLEX finite element modeling to assist in validating waveforms**

Using numerical analysis and developing models with same parameters can help to validate that the waveforms are real and the results that are obtained are genuine.

1.6 Structure of Thesis

This thesis has been organized in 6 chapters starting with Chapter 1 giving an introduction to the subject of interest and stating the objectives of this research. Chapter 2 presents a literature review on the theory and background used in this work. Chapter 3 presents the three point bend testing setup including sample preparation and the fabrication and mounting of sensors. Chapter 4 presents the set up and usage of the high-speed imaging system along with the experimental modifications leading up to the final experimental setup. The result from the three point bending test and numerical simulation are presented in Chapter 5. The thesis will conclude with an overall summery and future recommendation for this research in Chapter 6. The final section includes references and the appendix for this work.

CHAPTER 2

Literature Review

2.1 Failure Due to Fatigue

Published reports in the area of fatigue date back to the early 19th century. The first fatigue study is accredited to a German engineer by the name of W.A.J. Albert, back in 1829, where he studied the effect of repeatedly loading an iron chain. Fatigue failures occur in many different forms such as mechanical fatigue, corrosion fatigue, fretting fatigue, rolling and sliding fatigue, and thermo mechanical fatigue (Suresh, 2004). Research has progress rapidly since then but the fact still remains that majority of failures take place due to the influence of cyclic loading. As early as 1853, credible engineers such as Braitwaite and Mr. Field published work that introduce fatigue failure is actually due to cracks in the material. Loading and unloading a material at a certain level will cause microscopic cracks. Once a crack reaches a certain level that structure or sample will fracture. The amount of stress required to propagate pre-existing flaws (cracks) in a material became known as fracture toughness. Crack growth rates could now be expressed as a function of the stress-intensity factor range(ΔK). K incorporates the three main crack characteristics that are involved with crack propagation; crack size, stress, and geometry. K varies widely for different materials and is affected by temperature, loading rate, and secondly by the thickness of the test specimen [9]. One of the most notable equations regarding crack growth is given by:

$$\frac{da}{dN} = C(\Delta K)^m$$

where *a* is a representative crack length, *n* is the number of fatigue cycles, ΔK is the applied stress intensity factor range, and *C* and *m* are assumed to be constants for a particular material. This equation can also be written in log form. Expressing da/dN as a function of ΔK puts the

results in such a form that they are independent of planar geometry. This allows the data to be interchanged and used for comparison of data obtained from a variety of specimen configurations and loading conditions.

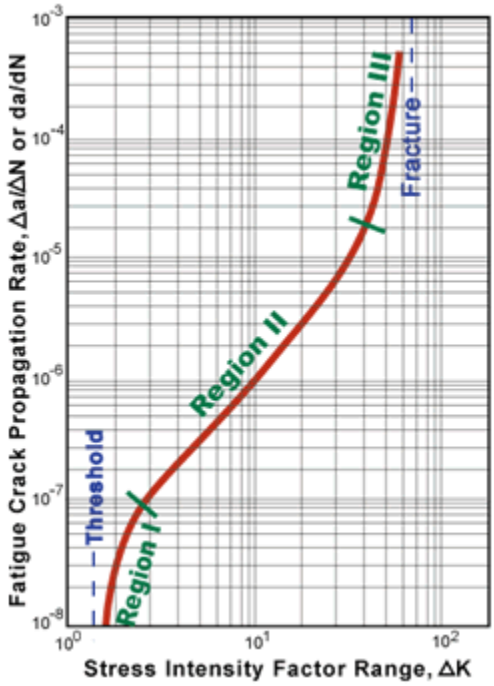

Figure 3. Stress intensity vs. crack growth rate

In the figure above, region I represents the relationship of ΔK being too low for the crack to propagate. In region II the crack change is linear with the change in ΔK and in region III, the crack growth changes in large amounts with little change inΔK. To increase the distance at which the crack propagates, literature introduces an overload method shown in the figure below.

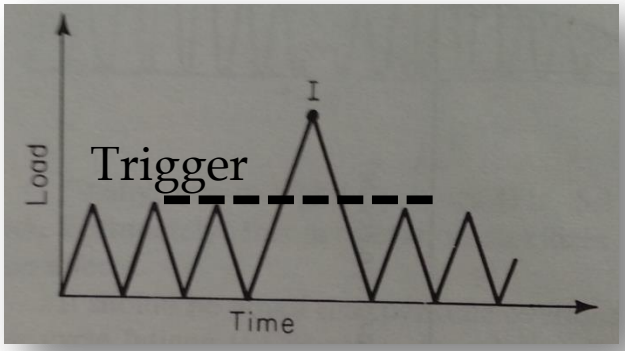

Figure 4. Overload method

The overload method increased the crack velocity, which would increase the distance at which the crack propagates if loaded with the same frequency. Immediately afterwards the crack goes into retardation phase were the specimen must be load until the crack sharpens and the created secondary phase out grows the primary phase. This technique may be useful for growing larger cracks along the surface to be capture with the high speed imaging system.

There are several tension testing techniques that are used for crack propagation; three point bending will be the focus of this section. The ASTM standard E1290-08 and the Bower equations to determine the stress intensity factor for specimens under three point bend testing are nearly identical. This study will use Bower's Equation, given by:

$$K_I = \frac{4P}{B}\sqrt{\frac{\pi}{W}}\left[1.6\left(\frac{a}{W}\right)^{\frac{1}{2}} - 2.6\left(\frac{a}{W}\right)^{\frac{3}{2}} + 12.3\left(\frac{a}{W}\right)^{\frac{5}{2}} - 21.2\left(\frac{a}{W}\right)^{\frac{7}{2}} + 21.8\left(\frac{a}{W}\right)^{\frac{9}{2}}\right]$$

where P is the applied load, a is the length of the crack, B is the thickness of the specimen, and W is the width of the specimen. Three point bending is method that can provide information such as flexural strain, flexural stress, and flexural modulus. This method can also be used to determine the fracture toughness of a specimen. The goal is not to completely fracture the

specimen but to propagate a crack at length great enough to view on the surface and capture it across several frames in a video.

2.2 Crack Growth in Thick Aluminum Samples

Of the multiple AE sources, crack growth is one of the few that can be detected, located, monitored, and physically seen. In nature, crack propagation is random and can occur during anytime a system is in operation. Through fatigue analysis engineers can determine where the most gullible areas to cracking are located; therefore, sensor location can be better placed for detection. Once the crack is detected and located, the next step is to quantify the crack. ASTM standard E647-13e1 covers several ways to measure the size of the crack; by compliance, electrical potential difference, and by what is used in this study, visual measurement. Over the past few years the focus has transferred from AE source location to having the ability to control and monitor crack propagation.

Crack propagation in thick samples is more complex and complicated than that of thin samples. Joel Schubbe studied crack growth behavior in respect to grain orientation for thick specimens (Schubbe, 2009). His results indicate that crack growth behavior depends on the grain size orientation. Grain orientation depends on production method of the material. Depending on the direction that aluminum is cut and laid determines it physical capabilities and material properties for that certain direction. The figure below shows the material morphology in aluminum.

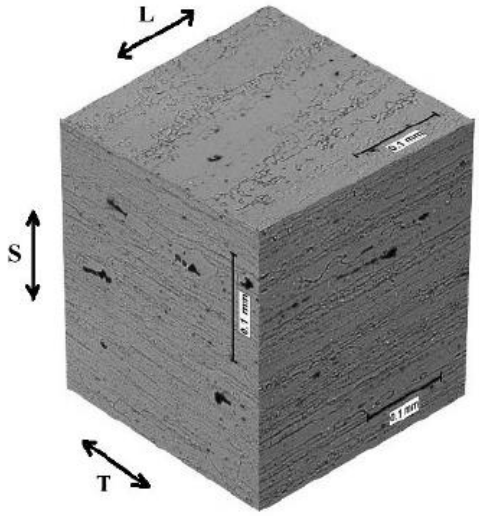

Figure 5. Material grain direction

Results in Schubbe study indicate that T-L data show a higher increase in ΔK over L-T data, as predicted by thin material analysis. The most notable extract from the results was the increasing retarded crack growth rate once the ΔK surpassed a certain level. Over a certain level, the crack tends to have a splitting or branching effect which greatly impacts the growth rate. There is also a direct correlation between the flight hours, crack length, and crack growth rate. As the service life of thick materials increase, the crack length increases, as well as the growth rate (m/cycle).

Another study done on thick aluminum structures also studied the effects of grain orientation (Wei et al., 2013). Accredited by multiple sources, they found that there is an improvement on the fatigue life of thick plates compared to thinner plates, shown by the S-N curve. This is primarily due to the fact that less densely particles in thick plates reduce the chance to induce cracks. They also showed that with increasing the stress during fatigue loading that initiation of the crack is about 200μm or more from the free surface. Because crack initiation is away from the free surface, more constituent particle or defects in the material could become potential crack initiations. This could cause multiple crack growth sites, which would indicate

that the main crack is growing into or joining the other cracks. They also propose that in thicker specimens that cracks tend to grow along different crystallographic planes in different grains. This may be an issue as the crack could possibly grow in multiple locations in the interior and not propagate along the surface at the same rate.

2.3 Acoustic Emission in Fatigue Analysis

The crack growth rate equation described above is greatly accepted in the AE society. Some attempts have been made to relate AE signal characteristics such as the amplitude and event counts to particular events occurring in the material. As seen in (G.J. Hancock, 2003) they propose an equation that relates AE count rate to K.

$$\frac{d\eta}{dn} = B(\Delta K)^p$$

Where h denotes the number of counts and *B* and *p* are assumed to be constants for a particular material. This equation may be at advantage for procedure to calculate and determine the stress intensity factor becomes less complex.

A general assumption is that crack growths occur close to maximum peak loads. As declared by Moorthy et al. in their investigation, "ductile crack growth is a very weak source of acoustic emission and that during fatigue crack growth damage is not induced by the maximum stress intensity factor, K_{max} but by the stress intensity factor range, ΔK." This notation clarifies that AE event may occur during anytime of the fatigue cycle, therefore, if one is looking to study AE events from all AE sources then all information must be acquired during the full cycle. Fretting is a source caused by a material grinding or rubbing against one another during operation (friction). While crack growth is in effect, fretting may also generate acoustic emission events. When loading the specimen, the crack face may grind against one another during crack

opening and by the creation of new surfaces and the possibility of debris, fretting will most like occur when the crack is closing.

2.3.1 AE Signal Characteristics A general acoustic emission signal is displayed below in Figure X on a voltage vs. time plot. Some of the characteristics are described and later used for analysis.

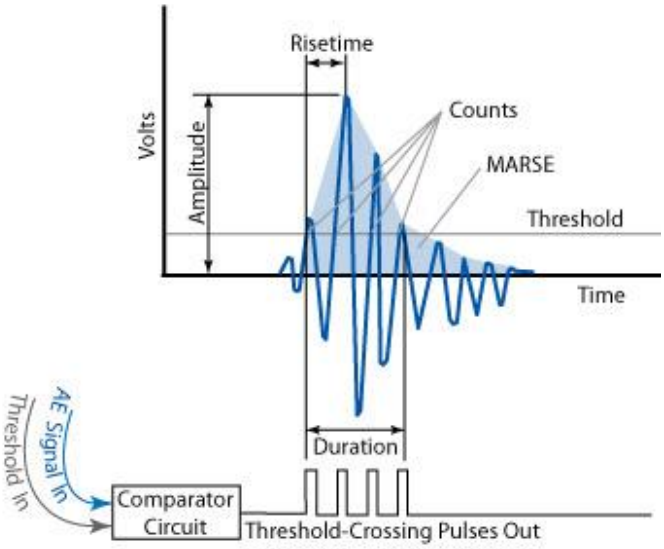

Figure 6. AE waveform

Amplitude -the greatest measured voltage in a waveform and is measured in decibels (dB).

Rise time - the time interval between the first threshold crossing and the signal peak.

Duration - the time difference between the first and last threshold crossings.

MARSE - sometimes referred to as energy counts, is the measure of the area under the envelope of the rectified linear voltage time signal from the transducer.

Counts - refers to the number of pulses in the signal with amplitudes greater than the threshold. Majority of the AE signal waveform features are affected by the geometry of the material, the source from which it was generated, the sensor characteristics, and the data acquisition system used.

2.3.2 AE Source Location Due to the numerous types of AE sources that can be generated within system, it is priority to have the ability to locate the source to eliminate the information from the unwanted sources and to only focus on the isolated source of focus. A number of works on AE source identification have been published and accepted amongst foregoing researchers in the AE field. There have been multiple techniques discovered that have the capability of locating exactly where the AE source derived from. AE source location techniques are separated into two stages:

1. the measurement of arrival times from received waveforms
2. using these arrival times to determine the origin of the acoustic source

The simplest method is bonding two sensors to the surface of the sample and differentiating the time of arrival of the signal. If the difference between the arrivals times are less than a micro second, it is evident that source is located in the center of the two sensors. If the location of the source is known, then the velocity of the wave propagating from the source can be determined. The downfall to this technique is the source location can only be determined in one dimension. The best-matched point search method to locate AE sources in 2D and 3D media may be a better method which was further developed into a two-step simple numerical approach: point generation and point matching. For point generation the specimen geometry is represented by an array of points with spatial location vectors. The point matching stage takes the array and searches for the best match to the experimentally measured time difference values (Scholey, et al., 2009). The simple method is efficient enough for this study due to the digital imaging supporting the visual aid of identifying crack growth as the AE source.

2.4 High-Speed Imaging

References are rare for using high-speed imaging to calculate crack growth velocities induced by three point bending test in thick aluminum specimens. However, there has been research that recommends sufficient frame rates that are reliable to capture crack growths. X.M. Li2 and F.P. Chianl used a high-speed camera in conjunction with a copper vapor laser to study the effects of subcritical crack growths in response to change in grain size in aluminum samples (Chiang, 1990). They ran a tensile test on single notched pure aluminum samples than was monitored by a high-speed camera and laser system to capture and analyze the dynamic fracture process. They later conclude that crack propagation was very much influenced by the microstructure of a material but what is important is the information regarding the high-speed imaging. Using two separate camera frame rates, 200 and 500 fps, they were able to study fringe patterns and estimate velocity due to strain components and strain rates. This frame rate does not capture the growth of the crack; therefore, the true velocity of crack growth was not captured. Instead, they use position of the crack that was captured within a frame to estimate a velocity but not knowing when it actually started and stop takes away from the accuracy of measurement.

An article submitted into the 5th *International Conference on Mechanical and Physical Behavior of Materials under Dynamic Loading*, analyzes the failure conditions of material 17 MoV 8 4 (mod) using a high-speed image converter camera. The experimental aim was measure crack propagation in specimens that were already pre-cracked. Using a 1:1 image lens, there was no clear crack visuals seen during recording; only after microscopic measurements were taken, where they able to determine the location and length at which the crack propagated. After a few trials the report claims that crack propagation was captured using 100,000 frames per second. Not only was it captured but they were able to pin point the exact frame at which this crack

growth occurred. From this point they were able to successfully grow the crack over several millimeters and capture its growth using 2 million frames per second, over a range of 18 frames. Although determining crack velocity and comparing this parameter to signal characteristics was not the focus of this article, it shows that crack propagation can be observed using higher frame rates for the particular set up used. Although no specific details where giving on load values, nor the type of dynamic loading, some of the information given in this report will be very helpful

CHAPTER 3

Three Point Bend Test

3.1 Introduction

Three point bending is well known testing technique for the study of crack propagation. The standard for this test is discussed in the previous chapter. This technique was used in this research for the following reasons;

- Three point bending localizes crack initiation for the convenience of visualizing crack growth monitoring by the imaging system along with the lighting system.
- The crack tip position remains in the field of view during testing.
- The set up can be easily altered to handle higher loads for thicker samples

The following sections describe preparations, parameters, and steps used in this experiment.

3.2 Sample Preparation

This section describes how the samples were altered and prepared for testing. The bar samples are made of 7075-T6 aluminum with the dimensions shown in the figure below. A starter notch is put directly in the middle of the length, along the entire thickness of the sample with the depth of 2.54mm (0.1in). The blade used to integrate the notch has a thickness of nearly 1mm. The notch is then sharpened with a standard razor blade to bring the notch to a sharper point to assist with enabling crack initiation. Then a 76.2mm (3in) section along the entire front surface and centered along the length was polished. Polishing was done using 3M sandpaper by systematically increasing the grit size from 150 to 2000. This gives a level, scratched removed surface in the area of interest. This type of polish did not provide enough contrast or lighting to visibly capture crack growth, therefore, later samples where improved by two different methods. Once the above process was complete, one sample was painted with a very thin layer of white paint and the other was polished using 6 micron diamond solution for a mirror like finish. The

samples were then ready for crack initiation process. After the crack was initiated, sensors were placed on the sample for the detection of AE events.

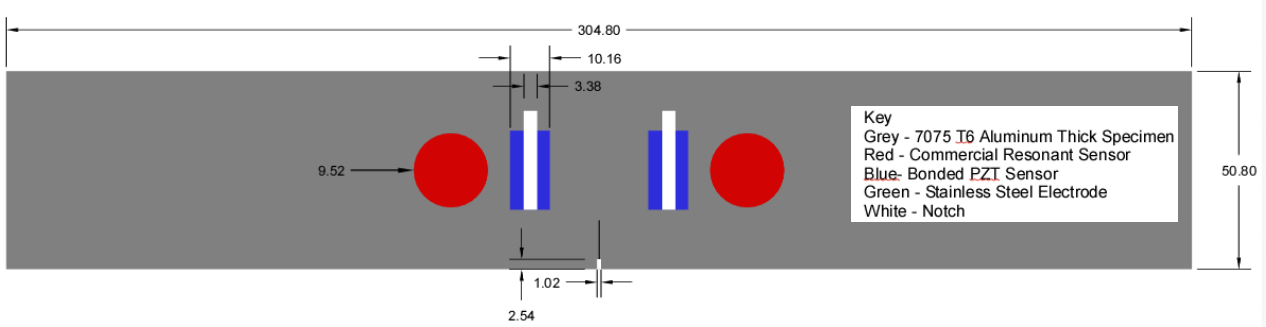

Figure 7. Schematics of specimen and sensor placement

3.3 Fabrication and Mounting of Sensors

` Fabrication of the bonded pzt sensors starts with etching away the nickel electrode coating on both ends of the top surface of the10 mm × 20 mm piezoelectric wafers. The wafer was then dipped in water to remove the excess etching substance. Both sides of the wafer were then cleaned with trichloroethylene by only wiping in one direction. Once the location of the wafer was marked on the sample, that area was sanded to create a rough surface and then the wafer was outlined by kapton tape, leaving the wafer free for movement. An additional piece of tape was then placed over top of the wafer and firmly pressed to completely seal the top surface. Super glue was then placed within the boundaries of the tape outline and the wafer was placed on top of the glue. Now that it is set in place, a thin piece of rubber and some type of weight was placed on top of the wafer to create the thinnest bond possible between the wafer and sample. This was then left for 2-3 hours to allow the glue to cure. Four mm strip aluminum was then cut to be placed on the un-etched surface of the wafer. The aluminum strip was also then sanded and solder was placed on one end of the top surface. Once the glue dries and the wafer is in place, the tape was removed from the top surface of the wafer. More tape was then placed on top of the

wafer only covering the etched surfaces. The aluminum strip was then placed on the wafer in the same manner the wafer was placed on the sample. Another piece of aluminum was then cut and sanded to be used for ground. The area on the sample where the ground would be located, which is close to the solder end of the aluminum strip, was also sanded to create a rough surface. Solder was also placed on the aluminum ground piece and then it was glued to the sample. Once the ground was bonded, the wire was soldered to the aluminum strip and the ground. It is very important to test the sensitivity and response of the sensor. If an abundance of noise is detected simultaneously or some other irregularities are observed there is most likely a ground problem or a there is an issue with a bond. In the case of a bond not being sufficient, the sensor should be completely removed and replaced.

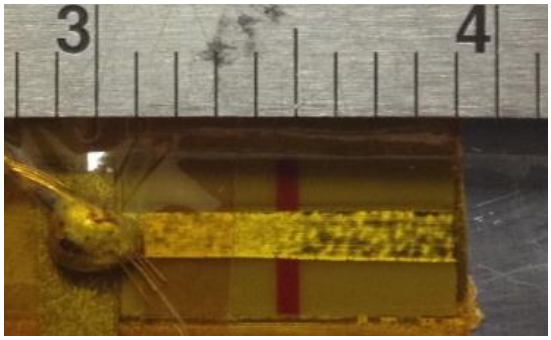

Figure 8. Bonded pzt sensor

3.4 Experimental Setup

The test set up uses four different systems during operation. It starts with the MTS system loading the specimen, the oscilloscope then triggers the high-speed system, the high-speed imaging system then records the crack growth along the surface of the material, and then simultaneously, the AE data acquisition system detects and records AE signals. The figure below shows the schematic of this experimental setup.

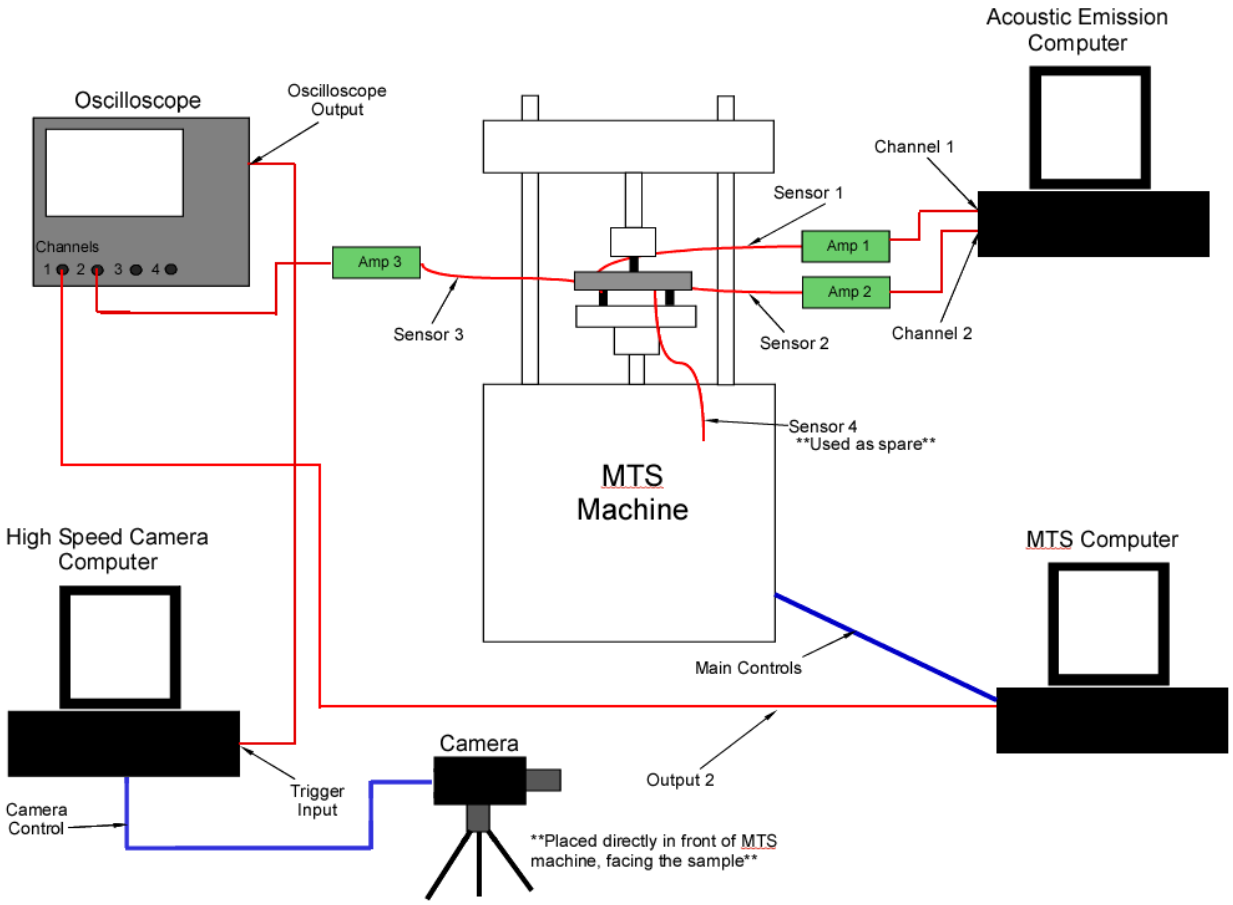

Figure 9. Testing setup

All parameters and settings for the MTS machine are set by the MTS computer to control the loading and unloading of the sample. There is also a bnc output cable from the MTS computer that attached to the oscilloscope to synchronize triggering the camera at certain load levels. The oscilloscope takes the load at which the MTS is operating, converts it into voltage and outputs a signal to the camera to trigger for recording by connecting the output cable from oscilloscope, to the trigger input of the high-speed camera computer. The camera is mounted on two translation stages, which is connected to an adjustable tripod and placed directly in front of the MTS machine so that the surface of the material can be easily viewed. The camera is controlled parameters set the high-speed imaging computer but is ultimately triggered by the oscilloscope. Finally, sensors are placed on the front surface of the sample to collect signals generated from

AE events. The pzt sensors are connected to amplifiers, which are connected to the AE computer to monitor and record AE events. During two condition triggering a sensor bonded to the specimen is connected an amplifier which is connected to the oscilloscope for triggering. This is the foundation and basic set up for testing; all alterations and modifications will be discussed in the next chapter.

3.5 Parameter Settings

The compressive testing of the bar samples were carried out using the 810 Material Test System (MTS). This system has the capability to provide load up to 20,000 lbs. of force. All tests were performed at room temperature. With the top bar located directly in the middle of the specimen and the lower bars where located 101.6mm (4in) from the center, the specimen is evenly loaded. The settings for crack initiation, crack tip sharpening, and cycle overload are displayed below. All testing parameters are controlled by MTS software.

Table 1

Parameter settings for the different types of three point testing

	Set point	Amplitude	Frequency	# of Cycles
Crack Initiation	-2600	1800	0.50	$> 20{,}000$
Crack Sharpening	-2200	1800	0.50	150
Overload	-2800	2200	0.04	1

Before testing, samples were centered on the three point bend fixture with single layer clothes located between the bend bars and bar specimen contact areas to reduce noise levels. Additionally, each pre-amplifier was grounded to the MTS machine. Once mounted, all tests where loading using the profile of a tapered sine wave.

CHAPTER 4

High-Speed Imaging and Experimental Modifications

4.1 High-Speed Imaging

All video was recorded using a Photron Fastcam 1024 PCI high speed camera with specifications of 100KM and 2GB. The camera was mounted on a two axis translation stage which was then mounted on an adjustable tripod stand. The camera was equipped with a 5 - 20x magnification objective lens connected to a magnification tube extender. Placed directly in front of the MTS machine, the objective lens could come with in millimeters of the sample. With the lens being perpendicular to the specimen, it can easily image the crack. The legs of the tripod were placed on thin rubber mats to help with damping normal vibrations from the MTS machine and surrounding instruments in the testing facility. The software capabilities for this system are displayed below.

Table 2

Camera capabilities

Photron Ver.338	
Frame Rate	60 – 109,000 frames/sec
Resolution	(max)
Shading	Calibrated
Partition	1
Shutter	Default or Custom
Trigger Mode	Manual, Center

Before any changes to settings, the shading was calibrated at the lowest frame rate and highest resolution for the best quality at higher frame rates Due to memory issues, high-speed imaging

cannot record long periods of time, and therefore, a specialized external trigger technique was customized for this experiment.

4.1.1 Triggering The time frame for which a crack propagates is a very small window; therefore, the camera must be triggered during a very specific time period. This dual condition trigger is controlled and monitored by an oscilloscope. An output from the MTS Output 2 was connected to channel 1 of the oscilloscope and the output from the sensor amplifier was connected to channel 2. The manual trigger input from the high-speed camera operator was connected to the output of the oscilloscope. The schematic below shows the settings used to setup the oscilloscope trigger:

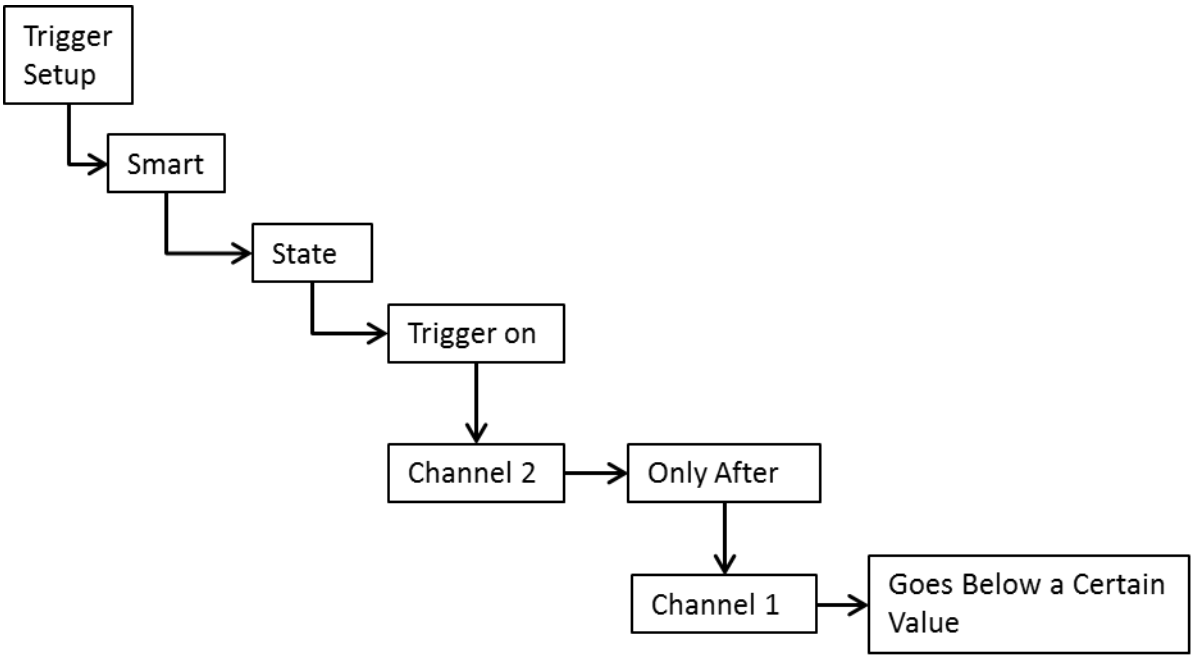

Figure 10. Two condition trigger.

The camera trigger was set up to only record when the load is below a certain value and an AE event occurs that crosses the Channel 2 trigger threshold. For the oscilloscope to actually trigger the camera, the BNC setup under utilities was set to trigger output on trigger out.

Triggering during an overload cycle is a little simpler. Depending on a signal is not needed for an overload because once the previous maximum load is surpassed the video begins to record, therefor, the camera is triggered at a certain load value, set by the oscilloscope. The trigger mode is also set to “start and not “center” because previous frames before recording is triggered is not needed.

4.1.2 Lighting Lighting for high-speed imaging is a system within itself. Lighting plays a critical role for cameras at higher magnifications. Additionally, recording at higher frame rates causes for high intensity lighting. Simple led lighting is insufficient for illuminating the sample surface during high-speed imaging. This experiment uses the ARRILUX 125 watt lighting system for illumination. This system adds a range of lighting options for testing. With adjustable focusing and intensity, this single system can be used for lower and higher frame rates. Due to noise induced by this lighting system, it must be powered from a separate source to significantly decrease the noise levels.

Figure 11. Lighting system

4.2 Experimental Modifications

Due to noise levels, contrast issues, and other variables that affect the outcome of normal test operations, specific changes and modifications where done to account for the inconvenience. This section describes what those changes are, as well as their importance.

4.2.1 Trial 1 Samples used during these test where polished only using sand paper ranging from 160 to 2000 grit. This would bring all of the scratches on the surface to same level which would provide a polish suitable enough to visualize crack growth. The imaging system was used at 60 frames per second at 20x magnification and was manually triggered. The lighting system at this time was simply a hand held LED flash light. AE event signals were detected us resonant sensor that was mounted to the surface.

The current settings did not allow for a crack growth to be captured. Cracks grow at a very high-speed; therefore, a much higher frame rate was needed. Another issue arisen during tests as it was seen that the sample quickly transitioned in and out of focus as the sample was being loaded. A different triggering technique must also be put in place to make this experiment repeatable.

4.2.2 Trial 2 A new set up was developed using a high-speed imaging system provide by the Materials Branch of Wright Patterson Air Force Base. This system allows the frame rate to be increased between 1,000 and 100,000 frames per second and it also increases the chance of capturing a crack growth. The oscilloscope system was introduced into set up to assist in having the ability to repeatedly trigger the camera at certain AE signal amplitude or at certain load levels. There was also change from rubber padding to kapton tape to a thin machine shop cloth as a material being used for an insulator. The rubber padding and kapton tape where not durable during test that operated at high cycles. This is very important to acquiring AE signals because

contacts between the bend bars of the three point bending tool and the test specimen would create an uncontrollable amount of noise in the signal content.

In conclusion to the changes, it was evident from the captured videos that a pre trigger was needed for the high-speed imaging software to capture the frames before the camera was triggered. When triggered by AE signal amplitude, the event would have already occurred before the camera would begin recording due to the synchronization of the different systems. A better lighting system was needed because the lighting from the LED flashlight quickly became insufficient when the frame rates were increased. The issue with the amount of noise detected and durability of the fabrication material was fixed.

4.2.3 Trial 3 Increasing the frame rate requires higher exposure of light; therefore, the high intensity light was incorporated into the system. The light was sufficient but it proposed the issue of creating more noise in the system. The magnification was decreased to 10x to increase the quality of the video. Having the ability to accurately see the exact location of the crack tip is disabled but increasing the quality improves the chances of calculating an estimated velocity. The camera software was upgraded and a pre trigger function was now available for use in the software. Also, a two condition trigger was introduced at this time to increase the possibility of capturing crack growth when triggering off of AE signal amplitude.

The noised from the high intensity light was dramatically decreased when the light was powered by another source. 10x magnification increased the quality of the videos, but the resolution and contrast quickly became an issue at higher frame rates. This set up did not result in the capture of any type of crack growth event.

4.2.4 Trial 4 To increase the contrast and lighting issues, the area of crack growth intent was coated with a thin layer of white paint on one sample and another sample was polished using

a 9 micron diamond solution to create a mirror like polish. Additionally, reflecting aluminum foils were utilized to confine and focus the lighting near the crack tip. An increase in the length of the crack length was needed so a 25% overload was now applied as one cycle during testing. After each overload, the crack tip was sharpened by cycling and then an overload was repeated. The camera is now triggered only when the camera reaches a certain value, the load at which the overload begins. The frames per second was also decreased to 10,000 frames per second

This set up resulted in 7 video samples of the surface crack growth using both the painted and the polished sample.

4.3 Final Experimental Setup

The last section of this chapter describes the final settings and alterations used in this research. Going from the 2000 grit polished surface to the 9 micron diamond finish really increased the image contrast. The thin layer painted surface was ideal, but due to the elasticity of paint, it was difficult to determine the true velocity of the crack growth. The mirror like finished improved the contrast, clearly shows the crack tip, and also provides true crack growth velocity.

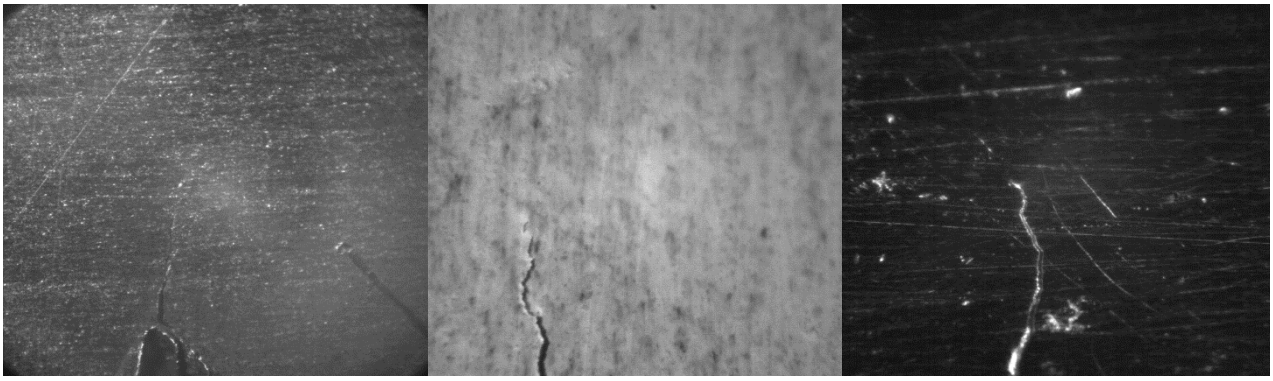

Figure 12. 2000 grit, thin painted, mirror like surface finishes

The overload technique was efficient enough to increase the change in crack growth length. The testing procedures for overloading changed multiple times. For example, the first overload procedures were as follows:

1. 150 cycles to sharpen crack tip
    a. Load varies from -400 ↔ -4000 lb.
2. Load sample to -4000 lb. to take reference picture
3. Start data acquisition system to record AE events
4. Overload sample for one cycle
    a. Load varies from -600 ↔ -5000 lb.
5. Load sample to -4300 lb. to take resulting picture

The frequency during the crack tip sharpening is the same as before, 0.50 Hz, and the frequency for the overload cycle is decreased to 0.08 Hz.

High-speed camera settings:

- 1000 Frames/sec
- Resolution: 512x512
- Shutter Speed: 99.09 μs
- Trigger Mode: Center (pre-trigger mode)
- Data Save Format: AVI
- Total Frames Recorded per video: 6400 frames

This procedure was carried out using resonant sensor for detection. The resonant sensors were replaced by bonded pzt sensors and the conditions were also altered. For test 1 through test 10 the following conditions were followed;

1. Load the sample to -4400 lb. and take reference picture
2. Start data acquisition system to record AE events
3. Overload sample for one cycle
    a. Load varies from -600 ↔ -5400 lb.
4. Load sample to -4400 lb. and take resulting picture

Each consecutive cycle was recorded during this phase of the experiment. The high-speed imaging settings where as follows;

- 10,000 Frames/sec
- Resolution: 128x256
- Shutter Speed: 99.09 μs
- Trigger Mode: Start
- Data Save Format: AVI
- Magnification: 20x

The crack was then sharpened using the crack sharpening method described in section 3.5 and for the next 10 test; everything remained the same except the high-speed imaging system was increased to 15,000 frames/sec in an effort to capture the crack growth extension across several frames. The loading levels and position of the camera altered over the final 10 tests. To get more light into the lens at higher frame rates, the camera system was positioned at an angle to the sample surface. This allows the camera to record up to frame rates as high as 100,000 frames per second. It also allowed the crack tip to be easily seen and monitored during growth. The changes in load levels are displayed in the results table

CHAPTER 5

Discussion and Future Research

The results for the final test are shown in Appendix A. Consistent loading conditions show a small percentage in change of AE events and the change in crack growth lengths. At 20x magnification, the camera focus can easily be affected by movement of the sample and vibration from other sources. Therefore, video quality for some tests is not clear enough to estimate crack growth velocity on the surface of the sample. At the given magnification and resolution, the field of view measures 0.21mm x 0.12mm. For test 1 through 20, the crack growth/cycle on the surface ranged from 0 to 0.019 mm and for test 21 through 30, there was an increase of maximum growth to 0.04. The frames reference images from which these measurements where take can be seen in Appendix B. Changes in the crack growth length smaller than 0.01mm are too small to calculate surface crack growth velocity due to the sudden change over such a small area. However, by knowing the frame rate, a minimum velocity can be calculated as if the crack propagated across one frame. A correlation between crack growth/cycle and the AE signals will be discussed later in the signal analysis.

Crack growth velocities along the surface must be proportion to the interior crack growths for a true correlation to be analyzed between crack growth velocity and AE signals. In thick samples, it is believed that crack initiations occur within the interior of the material before it propagates on the surface. One study claimed that crack initiations occur at a minimum of 200μm from the free surface (Wei et al., 2013). If this is the case then, the crack growth signals could potentially be coming from the interior crack growth and not that of the surface. Knowing the exact source of the acoustic emission is the solution to dilemma. As of now, I do not know of a distinct method to determine the difference between interior and surface crack growth signals

but there are patterns in the results that may indicate this type of behavior is being displayed in this experiment. During initial overload cycles, were the cycle was increased by 400lb., the amount of crack growth AE events show an increase in number but the change in the crack growth/cycle tend to be less than cycles were there was no overload and sometimes zero. This shows that some type of crack growth is occurring in the material but not on the surface being monitored. It is possible that the crack could be propagating on the back surface but the only way this could be determined is by having another imaging system in place to monitor the back surface during testing, which I did not have. When the same load was being applied to each cycle, the crack growth/cycle was very small and changed even though the testing conditions remained the same. Additionally, directly after the overload cycle, the same load type is applied to the specimen and the crack growth/cycle a dramatic increase but the number of crack growth events is the lease. It seems that the crack growth along the surface is not releasing enough energy to be detected by the sensors. By observation of these results I don't believe a reliable relationship can be developed to show a relationship between surface crack growth velocities and AE crack growth signals.

5.1 Signal Analysis

The backbone of AE is its capability to detect energy released from a source and convert it into a signal forms that can be viewed and analyzed. It is believed that signal characteristics can be used to relate information about the source from which it came. This puts us in the area of quantification. How can we use the information provide to us in signal form to quantify the event taken place in the structure? The AE events (signals) are broken up into three categories; crack growth events, fretting events, and other AE events such as noise.

Having the load history and time of arrival provides a simple way to distinguish between the three. If the signal arrives at one sensor during a time at which no signal has arrived at the other sensor, then this signal is classified as other AE event. The sensors are placed at the same distance from the center of the specimen. If the signal is generated by the crack, which is in the middle of the specimen, it will reach both sensors at the same time. When random events occur such as noise, then they tend to only be detected by one sensor. If one of the bottom bend bar becomes a source by contacting the specimen, then it also may only reach one source which would also classify it as other AE event. Crack growth and fretting events both arrive at the sensor at the same time. They difference between the two is that crack growth events occur within 5-10% of the maximum load while the load in increasing towards the maximum load and the crack is opening. Fretting events occur when the load is decreasing and the crack is closing. Most fretting events occur when the load decreases before heading the maximum load, but some may occur after the load has reached its maximum. The figure below shows the load profile and when the AE events can occur.

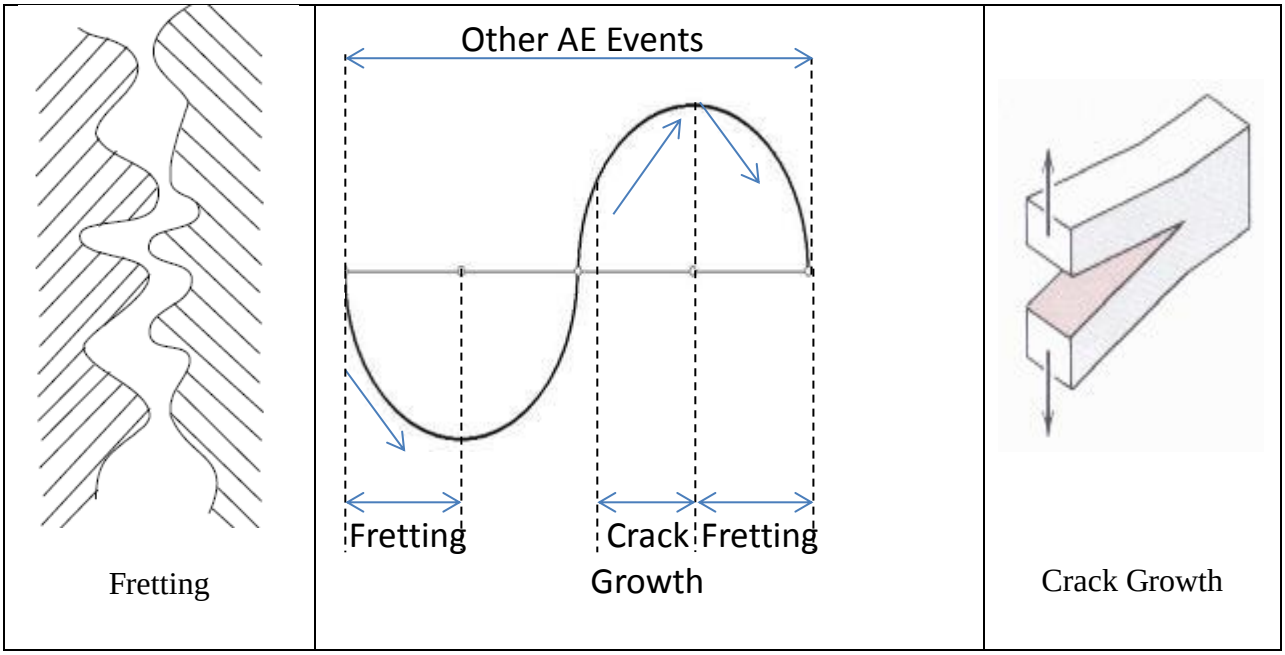

Figure 13. Fretting, load profile, crack growth

Placing the signals into these categories gives room for comparison and correlation between the signals. In a recent study, (Asamene, 2013) shows that 80% of fretting signals have a longer duration between the first and last points of crossing the threshold, than that of crack growth signals. He also concludes that the frequency content does not provide a basis of distinction as both crack growth and fretting events show a wide range of frequency content. This type of analysis will not be conducted here. In the next section I will attempt to build relationships between the type of event and the signal parameters.

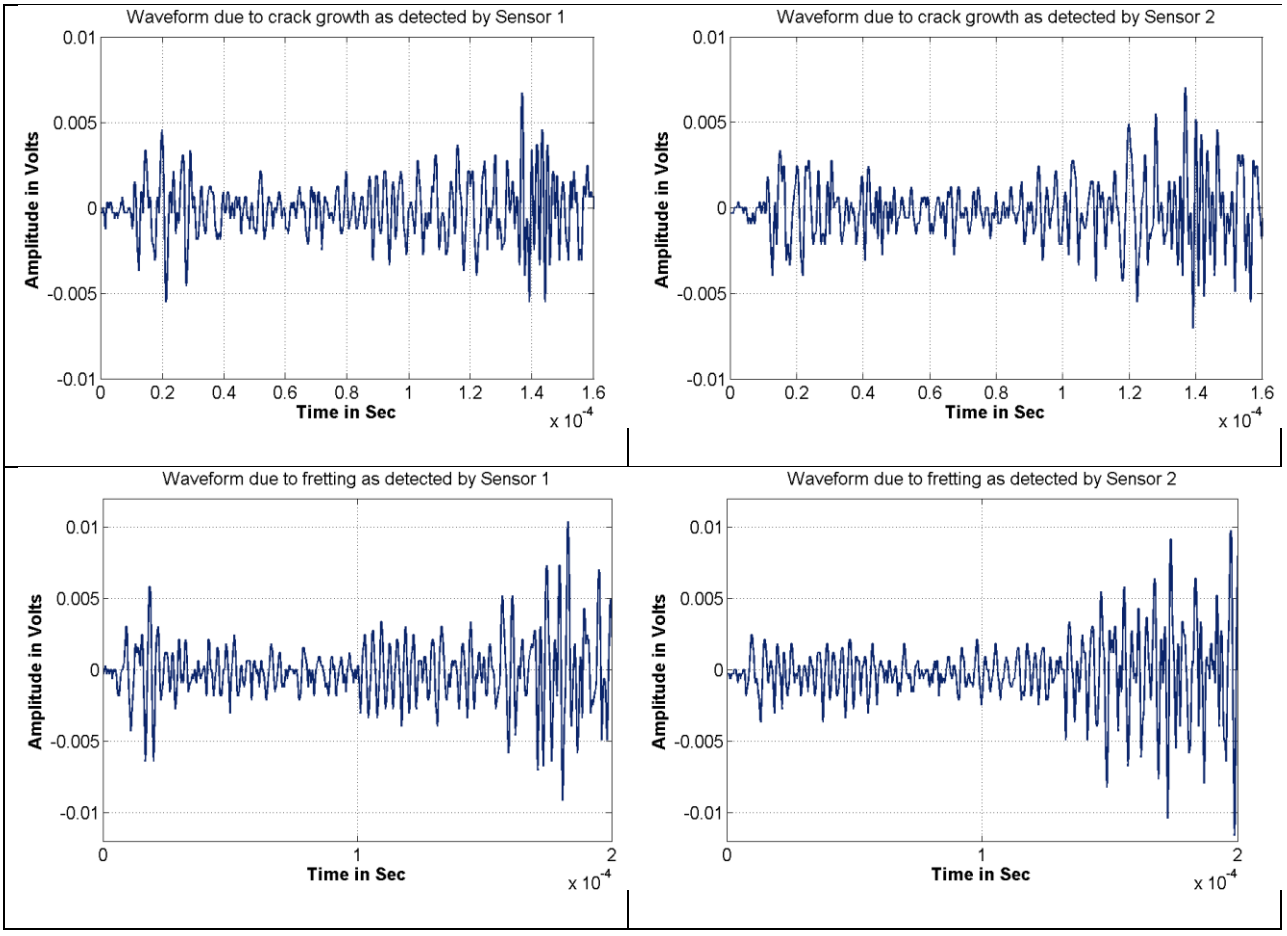

Figure 14. Crack growth and fretting AE signals

Sensitivity of the bonded pzt sensor was tested using pencil break test and results from test that showed one or multiple crack growth events and zero fretting or other AE events.

Amplitudes from a pencil break test showed similar amplitudes but amplitudes from the crack growth events average out to be exactly the same. From this I conclude that they both have a good bond to the specimen, with same or similar dimensions of all components. This is key, for signal characteristics should not vary much due to the sensor properties. Figure 11 shows that the characteristics for crack growth and fretting signals are very similar. Frequency content seems to the relatively close as well as amplitude, therefore time of arrival and the load at which it occurred is vital to distinguish the difference between the two. In theory, the greater the change in crack growth/cycle, the higher the amplitudes of AE signals and the count of crack growth and fretting signal detected would be higher. The figure below shows that there is no correlation between increase in crack growth/cycle and cracking, fretting, or other AE events.

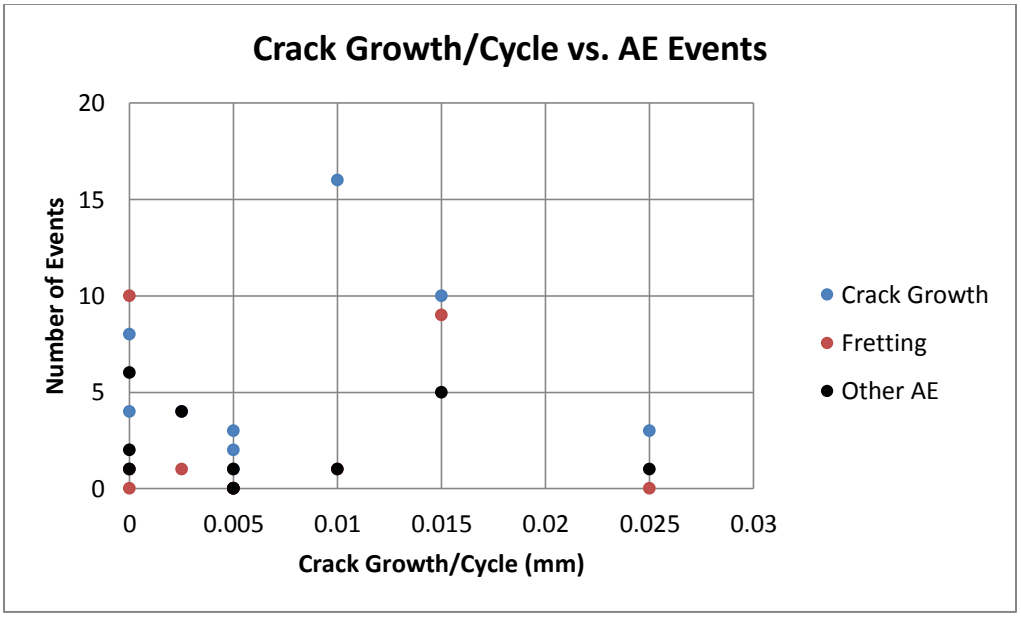

Figure 15. Crack growth/cycle vs. AE events

The next figure shows that no relationship shown between the load at which the crack events occurred and the maximum amplitude of the signals, although some of the higher amplitudes occurred at the higher load levels.

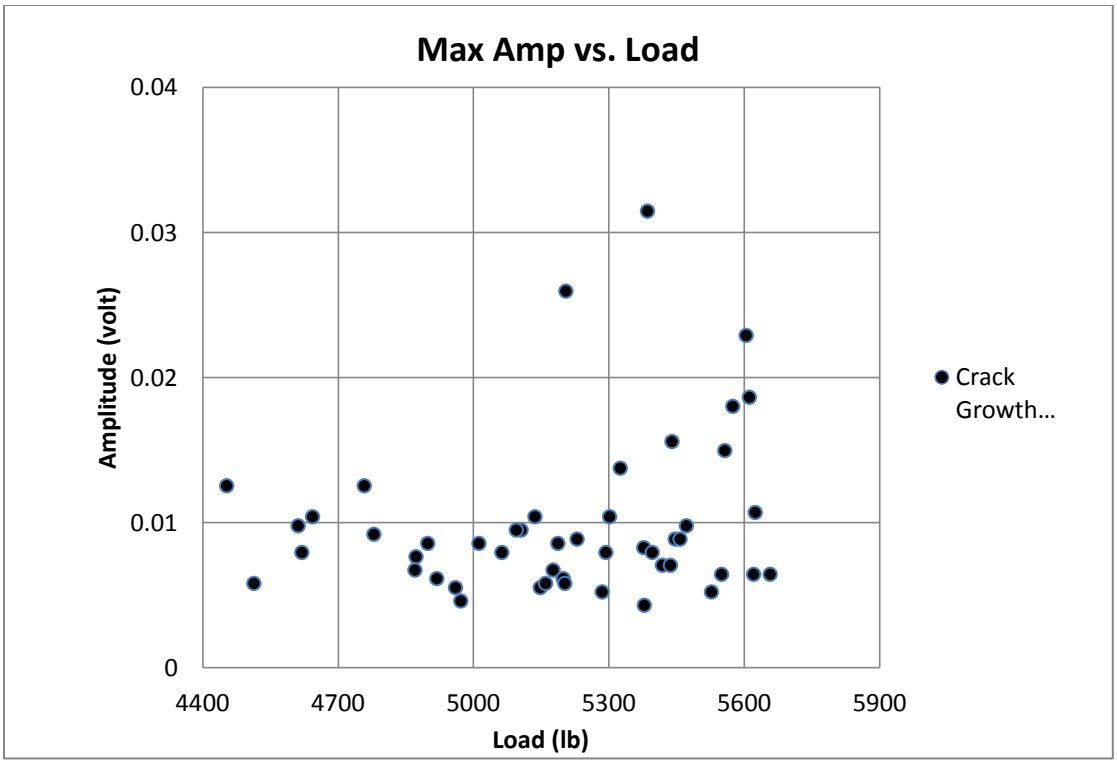

Figure 16. Maximum amplitudes vs. load levels

The next figure shows the effects of change in crack growth/cycle on the amplitude of the signals.

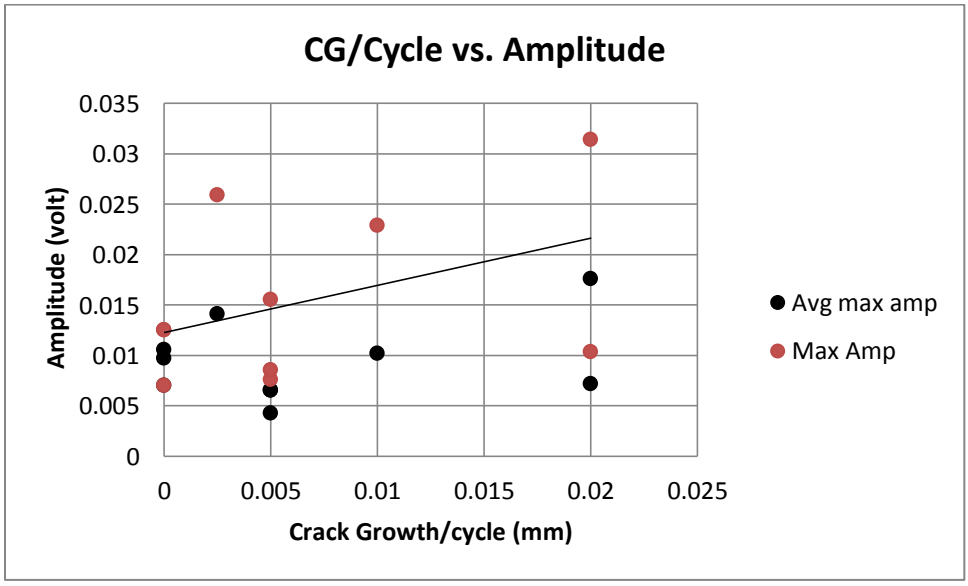

Figure 17. Crack growth/cycle vs. amplitude

Each cycle may or may not have contained multiple signals that are considered crack growth events. This correlation predicted before the experiments was that the amplitude levels of the signals would increase with the increase in the length of crack growth events. This figure shows this to be true all though it is not that strong of a trend between the data points. This is due to the minimum change in crack growth length per cycle. Longer crack growths would have released more energy; therefore, the amplitudes of the signals would have been higher. With this set up and testing conditions, the range of crack growth/cycle was between 0 and 0.4mm. The crack growth evolution can be seen below.

5.2 Interior vs. Surface Crack

The three point bending test was successful in propagating crack growth along the surface of the specimen. The surface crack has been measured to be 5.85 mm in length, the width varies do to the position, and the depth is unknown for the entire crack. The surface crack growth can be seen below in the figure. During early testing stages, the crack seem to be growing systematically, but in later testing the crack showed scattering and branching effects due to higher stress as stated by an earlier source (Schubbe, 2009).

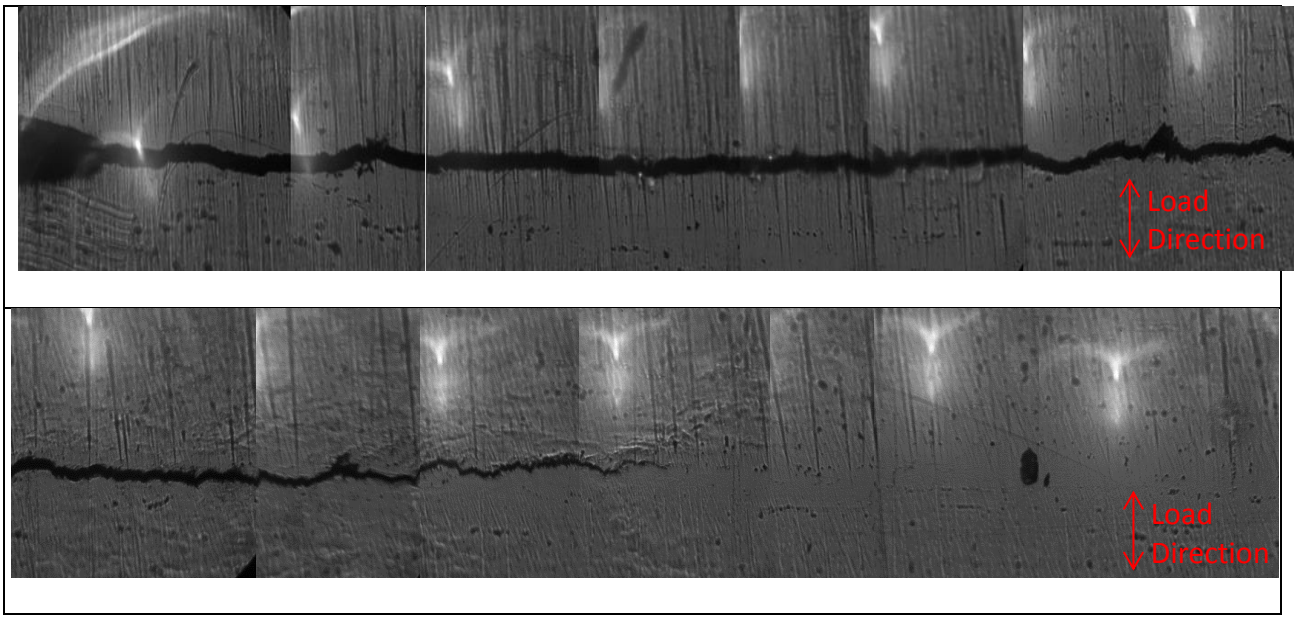

Figure18. Total length of surface crack

During the fatigue test process, two samples fractured. One fractured due to a rapid increase in load level and the other failed due to fatigue. Neither video nor the signals were collected during this event for analysis. The significance of this taken place is that the crack face is now visible and interior crack growth characteristics can be observed. What was believed was the interior crack grew with a higher velocity than that of the surface crack. This was not the case as seen in the figure below.

Figure 19. Outlined crack face of thick specimen

The area of crack growth is displayed as a more metallic surface then the rest of the material. The contrast between the two is hard to visualize, so the outline is placed there to show what was

seen under magnification. The bottom part of the figure shows the notch and the outline shows how far the crack had propagated. All four of the fractured specimens displayed this type orientation of the crack face of two peaks about a third and two thirds through the thickness and valley exactly in the middle of the two, in the middle of the thickness. The aspect of this type of crack growth behavior is not known but is understood with the use of plain strain and plain stress conditions. Due to the dimensions of the specimen, the interior crack growth propagates under plain strain conditions and the surface crack propagates under plain stress conditions due to the free boundary. This phenomenon does not explain the profile of the crack face, but it gives insight to why the interior has propagated further than the surface.

As this specimen is being fatigued, small features on the surface where being displayed that the crack eventually propagated into. It is believed that the propagation of the interior crack may be causing small cracks or dislocations on the free surface of the specimen. The figure below shows multiple features noticed during testing that channeled the crack on the surface of the material.

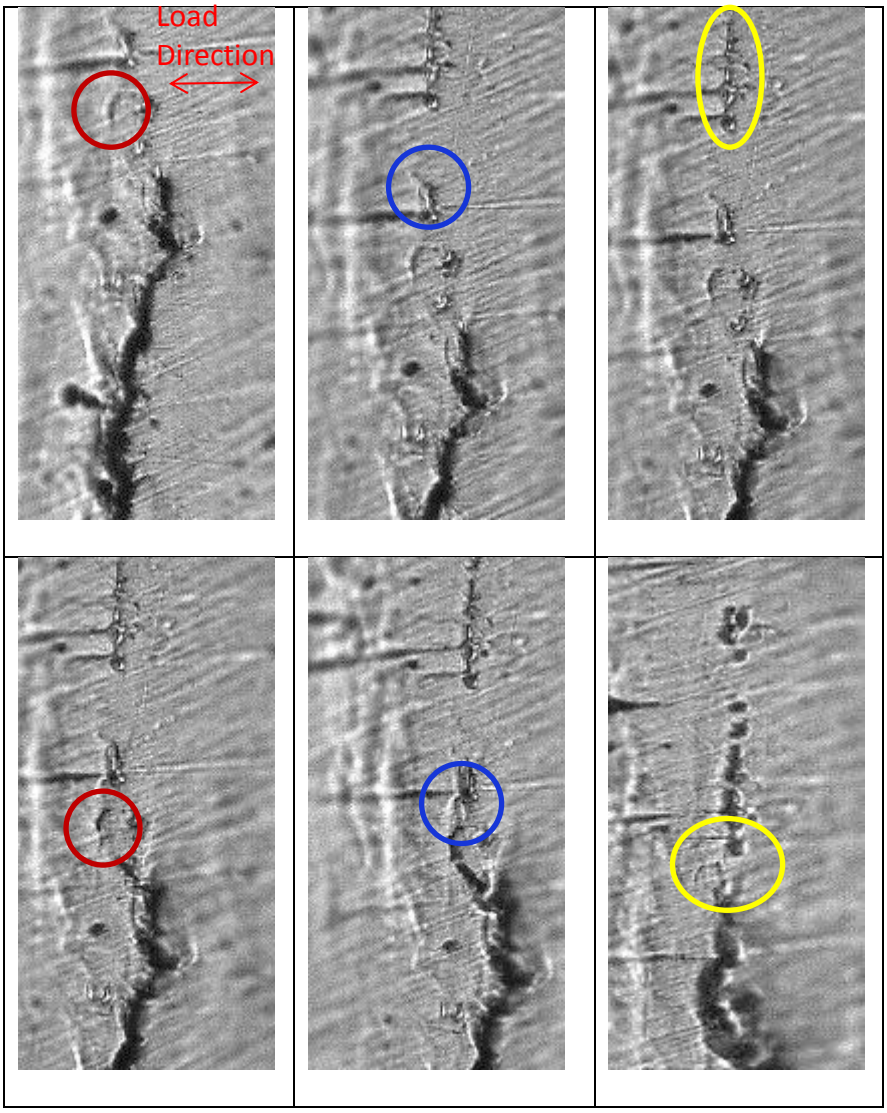

Figure 20. Surface features

The peak of the interior crack was measured to be 1mm above the crack tip along the surface of the material. At the current resolution, the interior crack would be four frames above what is being visualized.

5.3 Numerical Modeling

Finite element modeling program, PZFLEX is being utilized for numerical analysis for this study. The models are currently still being developed and modified to replicate this experiment; however, some results have been produced. Using a function developed by Hamsted, a well-known researcher in the AE field, is used a dipole source to drive the model.

The exact size of the specimen and specifications are used in the model along with the notch and three point bend bars.

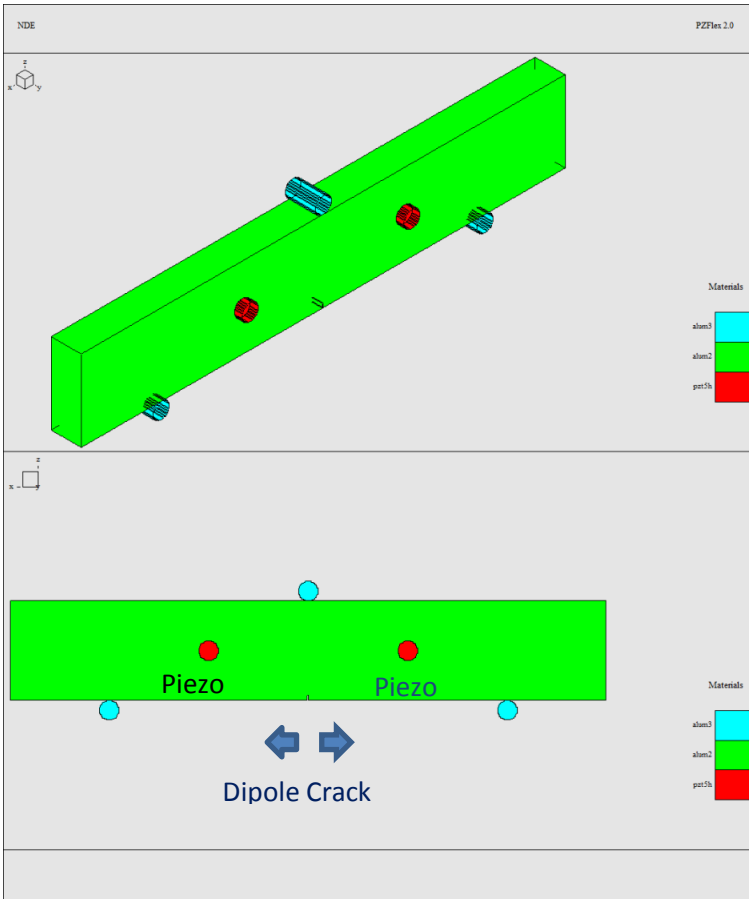

Figure 21. 3D model of specimen

The source represents a crack that grows through the entire thickness of the specimen with the same crack growth length. All nodes along this crack growth are excited simultaneously and the response of this structure is monitored by two pzt sensors that are also a part of the model. As can be seen in the signals below, the model signals look similar to the experimental AE signals. It is still unknown if this is the correct source to be used for AE. The model is currently being used to study signal characteristics for sources that are excited on the surface of the sensors, the interior of the specimen, and on the back surface of the specimen.

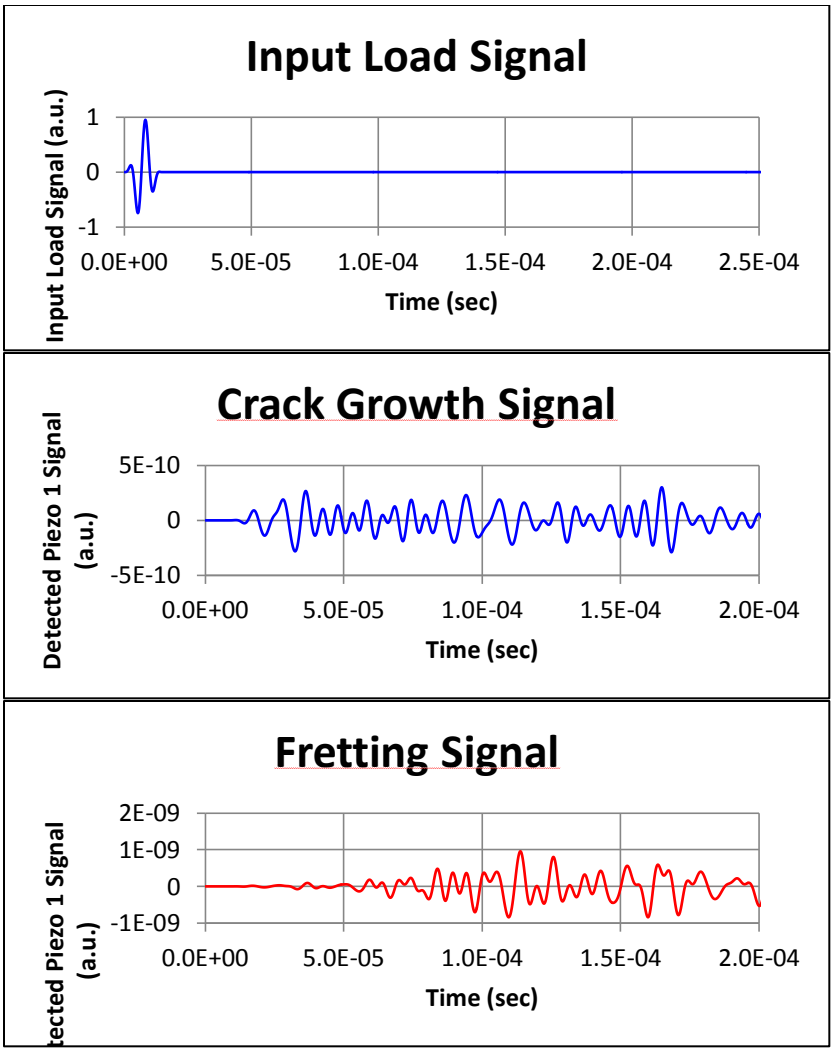

Figure 22. Numerical model results

CHAPTER 6

Summary and Future Research

In conclusion, I have developed a technique to accurately measure and correlate surface crack growths with AE crack growth signals. Majority of research done on the analysis of structures are conducted using thin samples for less complexity. The issues and objectives discussed in this study aim to advance the involvement and efficiency of AE in structural health monitoring. Using high-speed imaging and AE analysis, an effort was made to quantify AE signals to relay information about the source. The source of interest in this thesis is crack growth due to cracks are of a majority when discussing the failure of structures under fatigue. Experiments were geared towards propagating surface cracks in a thick aluminum bars so that it could be monitored by high-speed imaging and AE analyzing system. In addition to experimental results, numerical modeling will be utilized to help verify waveforms. The important results from the experiments are summarized below.

Notable Results

- By knowing the time of one frame and the length at which the crack extended, a minimum velocity of the surface crack growth could be propagated.
- A relationship between the crack growth/cycle along the surface and AE signal crack growth maximum amplitude show a distinct correlation. As the crack growth increased, the maximum amplitude increased as well. This goes to show that as the crack propagates over greater distance, more energy is released and detected by the pzt sensors.
- During overload cycles, crack growths/cycle along the surface tends to remain the same or go below average as the counts of crack growth signals tend to increase.

- Directly after the overload cycle, the crack growths along the surface showed the greatest increase but the count of crack growth signals decreased.
- From the fractured specimens, patterns show that the interior crack grows at an average location of 1mm above that of the surface crack.
- Distinct features on the surface of the material tend to channel the surface crack growth. These features are assumed to be caused by the interior crack growth.
- The assumed crack growth velocities should not be used to extract distinct characteristics from AE signals as it is not the true crack growth velocity and may be relating false information about the source.
- Numerical models show similar waveforms of AE experiments. It is believed that alterations of the source could lead to better understanding of crack growths.

As the objectives of this study was to find a correlation between AE signals and surface crack growths was not accomplished, notable findings were discovered during this study. The technique and methods used show difficulties and room for improvement as seen throughout the report. Below is discussion of future opportunities and advancements for this research.

Material

Having a more brittle material will decrease the possibilities of plastic zones and would increase the length of crack growth/cycle. The ideal material would be one that is transparent and brittle in the same sense. Having transparency would enable the possibility to see the crack face as well as the crack growth along the surface.

Extended Crack Growth

The surface crack growth extended in very small increments under the current conditions presented. It would of benefit to grow the crack at least 1mm or greater as it is predicted that

there would be more of a proportional growth between the crack growth of the surface and the interior giving a decrease to false positives.

Advancing Multiple Imaging Systems

The high-speed camera used in this experiment is outdated in da fashion that new technology has developed new software that increases the capabilities of high-speed imaging. Having greater frame rates and better resolution would increase the possibility and clarify surface crack growths on a micron level. Additionally, having another imaging system in place to monitor the back surface could use to validate the source. If there is no visual crack growth on either surface and crack growth signals occur then it could be assumed that interior crack growths occurred given AE crack growth signals.

Numerical Model

Using the numerical model to show wave characteristics from the sensor surface, the interior, and the back surface could validate waveform characteristics to help locate the source of AE. Comparing the numerical model to the experimental results may give insight to alterations of the source. It would be of benefit to advance the model, using it to show response of different crack orientation and possibly total fractures could help clarify some results.

Knowing specific information such as; knowing the exact source of AE or the parameters that would affect the source of AE, has the potential to save lives. Have the capabilities to detect, locate, and quantify cracks is a skill that will save time and money. Knowing that there is a defect is important, but knowing the specifics about that defect is of greater importance. This thesis gives insight to advancing the knowledge of AE and crack propagation to improve the skill of structural health monitoring.

References

Ares J. Rosakis, Demirkan Coker and Yonggang Y. Huang. (1999). Subsonic and Intersonic Dynamic Crack Growth in Unidirectional Composites (G. A. Laboratories, Trans.). Pasadena: California Institute of Technology.

Asamene, Kassahun. (2013). *Monitoring Damage Initiation and Growth in Composite Structures by Acoustic Emission Method.* (Doctor Of Philosophy Dissertation), North Carolina A&T State University.

Barter, Simon. (2003). Fatigue Crack Growth in Several 7050T7451 Aluminium Alloy Thick Section Plates with Aircraft Manufacturer's and Laboratory Surface Finishes Representing Some Regions of the FA-18 Structure. In D. P. S. Laboratory (Ed.): Defence Science and Technology Organisation.

Chiang, X. M. Li and F. P. (1990). Dynamic Study of Subcritical Crack Growth in Coarse-grained Aluminum (M. Engineering, Trans.) (pp. 1-12): SUNY College of Engineering and Applied Science.

D.M. Owen, S. Zhuang, A.J. Rosakis And G. Ravichandran. (1998). Experimental determination of dynamic crack initiation. *International Journal of Fracrure, 90*, 153-174.

Defense, Department of. (2013). Standard Test Method for Linear-Elastic Plane-Strain Fracture Toughness KIc of Metallic Materials (Vol. E399, pp. 1-33): ASTM.

Fangt, Avraham Berkovits And Daining. (1995). Study of fatigue crack characteristics by acoustic emission. *Engineering Fracture Mechanics, 51*(3), 401-416.

Fujimoto, Takehiro, & Nishioka, Toshihisa. (2010). Experimental and numerical study for crack propagation in aluminum alloy A2024-T351. *IOP Conference Series: Materials Science and Engineering, 10*, 012055. doi: 10.1088/1757-899x/10/1/012055

G.J. Hancock, M.A. Bradford, T.J. Wilkinson, B. Uy, K.J.R. Rasmussen. (2003). *Advances in Structures* (Vol. 1): A.A. Balkema.

HAMSTAD, M. A. (2007). Acoustic Emission Source Location in a Thick Steel Plate by Lamb Modes. *Journal of Acoustic Emission, 25*, 194-214.

J. T. Glass, S. Majerowicz, R. E. Green, Jr. (1983). Acoustic Emission Determination of Deformation Mechanisms Leading to Failure of Naval Alloys: Johns Hopkins University.

James R. Mitchell, D. M. Egle, and F. J. Appl. (1973). DETECTING FATIGUE CRACKS WITH ACOUSTIC EMISSION (a. N. E. Mechanical, Trans.) (pp. 121-126): University of Oklahoma.

Jonathan J. Scholey, Paul D. Wilcox, Michael R. Wisnom, Mike I. Friswell, Martyn Pavier And Mohammad R Aliha. (2007). A Generic Technique For Acousitc Emission Source Location. *Journal of Acoustic Emission, 27*, 291-298.

Karlsson, Linus. (2010). *Crack Detection in Welding Process using Acoustic Emission.* (Independent thesis Advanced level (degree of Master (One Year))), Mälardalen University.

Materials, American Society for Testing and Materials. (2013). Standard Test Method for Linear-Elastic Plane-Strain Fracture Toughness KIc of Metallic Materials1 (Vol. E399): ASTM.

Mohamed Shehadeh [1], Ibrahim Hassan [2], Hany Mourad [3], Hassan El-Gamal (2012). *Monitoring Erosion-Corrosion in Carbon Steel Elbow Using Acoustic Emission Technique*. Paper presented at the 30th European Conference on Acoustic Emission Testing & 7th International Conference on Acoustic Emission, University of Granada.

Palmer, I. G. (1973). Acoustic emission measurements on reactor pressure vessel steel. *Materials Science and Engineering, 11*(4), 227-236. doi: http://dx.doi.org/10.1016/0025-5416(73)90083-9

Pullin, Rhys, Eaton, M. J., Hensman, James J., Holford, Karen M., Worden, Keith, & Evans, S. L. (2010). Validation of Acoustic Emission (AE) Crack Detection in Aerospace Grade Steel Using Digital Image Correlation. *Applied Mechanics and Materials, 24-25*, 221-226. doi: 10.4028/www.scientific.net/AMM.24-25.221

Schubbe, Joel. (2009). *Fatigue Crack Growth in Thick Plate 7075 Aluminum*. Paper presented at the 25th ICAF Symposium, Rotterdam.

Servansky, Daniel Paul. (2012). *A Novel Approach to Data-Driven Modeling of Damage-Induced Elastic Wave Propagation.* (Master of Science in Mechanical Engineering), Drexel University.

Standard Test Method for Measurement of Fatigue Crack Growth Rates1. (2013) (Vol. E647): ASTM.

Suresh, S. (2004). *Fatigue Of Materials* (2 ed.). United States of America: Cambridge University Press.

Wei, Lili, Pan, Qinglin, Wang, Yilin, Feng, Lei, & Huang, Hongfeng. (2013). Characterization of Fracture and Fatigue Behavior of 7050 Aluminum Alloy Ultra-thick Plate. *Journal of Materials Engineering and Performance, 22*(9), 2665-2672. doi: 10.1007/s11665-013-0561-8

Appendix A

Three Point Bend Test Results

	Fatigue Testing Results						
Test Number	Maximum Load (lb.)	Crack Growth Events	Fretting Events	Other AE Events	Crack growth/cycle (mm)	Frames	Estimated velocity (mm/sec)
1	5400	1	0	1			
2	5400	1	0	0	0.0075	N/A	75.7
3	5400	1	0	0	0.0025	N/A	25.2
4	5400	2	0	0	0.005	N/A	50.5
5	5400	3	0	0	0.005	N/A	50.5
6	5400	0	0	1	0	0	0
7	5400	1	0	0	0.0075	N/A	75.7
8	5400	1	0	0	0.01	TBD	TBD
9	5400	1	0	1	0.0025	N/A	25.2
10	5400	0	0	2	0.005	N/A	50.5
11	5400	4	1	4	0.0025	N/A	38.02
12	5400	1	1	1	0	0	0
13	5400	1	0	1	0.005	N/A	76.05
14	5400	1	0	2	0.019	TBD	TBD
15	5400	1	0	1	0.01	TBD	TBD
16	5400	1	0	0	0.003	N/A	45.6
17	5400	1	0	0	0.006	N/A	91.3
18	5400	1	0	0	0.001	N/A	15.2
19	5400	4	0	2	0	0	0
20	5400	1	0	0	0.005	N/A	76.05
21	4400	1	7	0	0.01	TBD	TBD
22	4400	1	9	0	0.01	TBD	TBD
23	4800	8	10	6	0	0	0
24	4800	0	11	5	0.02	TBD	TBD
25	5200	10	9	5	0.015	TBD	TBD
26	5200	0	8	5	0.04	TBD	TBD
27	5200	1	1	0	0.005	N/A	76.05
28	5200	0	1	0	0.015	TBD	TBD
29	5600	16	1	1	0.01	TBD	TBD
30	5600	3	0	1	0.025	TBD	TBD

Appendix B

Figure B-1

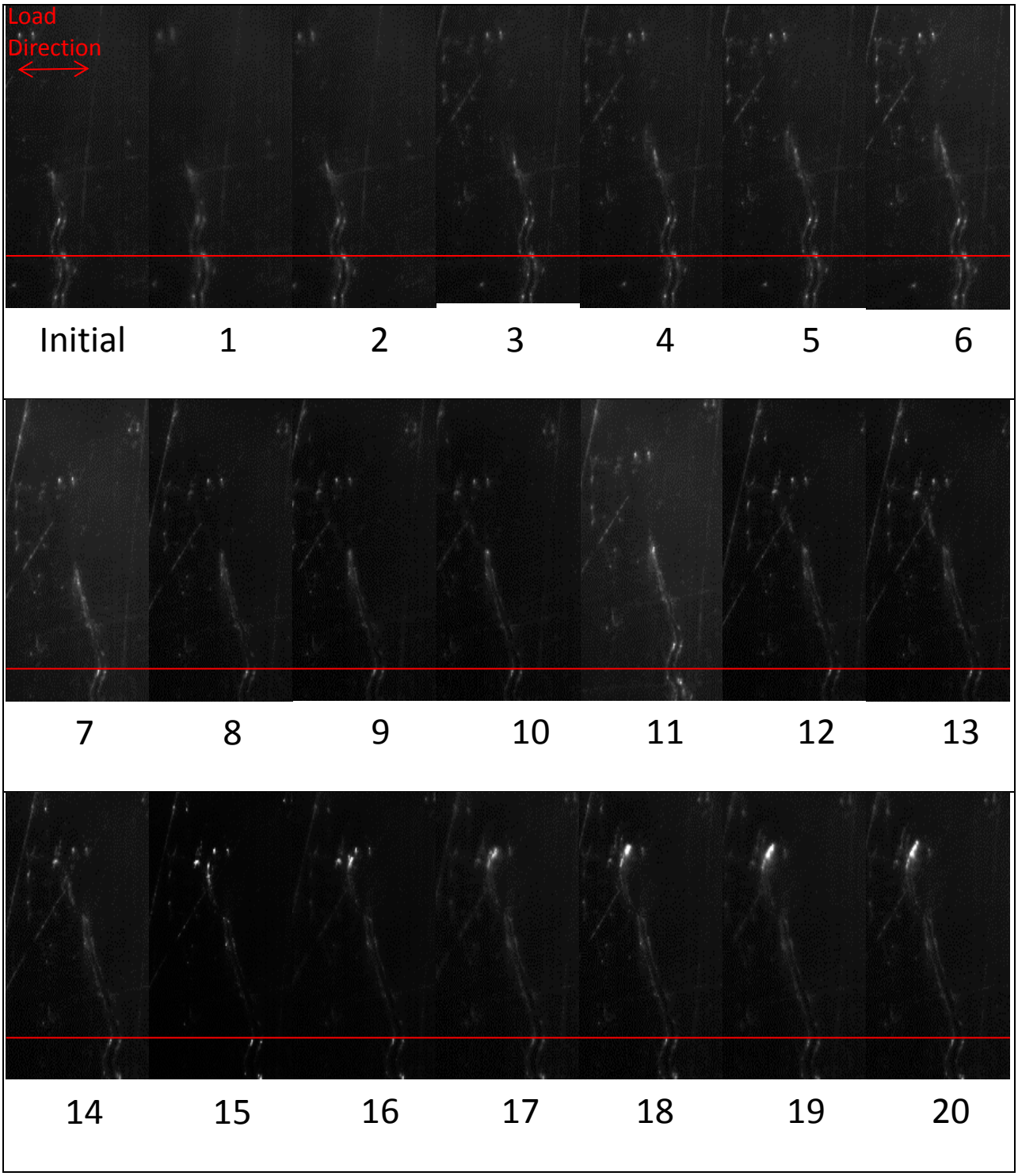

Figure B-2